



## Synthesis and physicochemical characterization of Arabic gum microgels modified with methacrylic acid as potential drug carriers

SANI M. IBRAHIM<sup>1,2</sup>, MISNI MISRAN<sup>1</sup> and YIN YIN TEO<sup>1\*</sup>

<sup>1</sup>Department of Chemistry, Faculty of Sciences, University of Malaya, Kuala Lumpur, Malaysia and <sup>2</sup>Department of Chemistry, Faculty of Sciences, Federal College of Education, Zaria, Nigeria

(Received 9 September 2021, revised 18 February, accepted 21 February 2022)

**Abstract:** Microgels of carbohydrate polymers are non-toxic and biocompatible that can readily be used in applications such as drug delivery, medicine, and pharmacy. In this work, Arabic gum (AG) microgels and methacrylic acid modified Arabic gum microgels (AGMAA) were synthesized via the water in oil emulsion polymerization technique using Tween 20 as the surfactant and hexane as the solvent. The microgels were characterized using various physicochemical methods such as Fourier transform infrared spectroscopy, thermal stability using differential scanning calorimetry, diffraction pattern analysis using X-Ray diffraction, morphology observation using field emission scanning electron microscopy and dynamic light scattering was used to analyze the size and zeta potential. The rate of deformation was higher in the AG microgels compared to the AGMAA microgels. The particle size and zeta potential of the AGMAA microgel were found to be larger and more negative than AG microgel, respectively. The particle size and zeta potentials of the microgels were found to be dependent on the amount of methacrylic acid as the modifying agent. The microgels were encapsulated with doxorubicin through the swelling method and the *in vitro* release was studied in mediums with pH values of 4.2 and 7.4. The results suggest the potentials of these microgels for drugs delivery.

**Keywords:** carbohydrate; encapsulation; drug delivery; doxorubicin; emulsion.

### INTRODUCTION

Biopolymers of polysaccharide origin are currently used in different biomedical domains for applications such as drug delivery and tissue engineering due to their cytocompatibility and degradation possibility without causing damage to the systems.<sup>1</sup> Most of these biopolymers require additional modification to overcome

\*Corresponding author. E-mail: yinyinteo@um.edu.my  
<https://doi.org/10.2298/JSC210909015D>

the problem related to mechanical instability resulting from exposure to different media.<sup>2,3</sup>

Generally, microgels are targeted at increasing the drug loading, promote slow release and reduce the side effects of drugs during delivery for the application in the biomedicine and pharmaceutical fields. Microgel synthesis from natural polymers, such as carbohydrates, have shown an increasing trend due to their promising nature for drug delivery.<sup>4</sup> They are generally non-toxic, biodegradable, biocompatible and possess tuneable properties including shape, size and porosity.<sup>5,6</sup> The distinct properties of microgels include biocompatibility, permeability and water retention capacity have led to different applications of microgels in biomedical fields such as wound dressing, tissue engineering and blood vessel replacement, contact lenses and drug delivery systems.<sup>7,8</sup>

Arabic gum (AG) is among the class of carbohydrates that have found various uses in adhesive, food, cosmetics, medical and other industrial applications. The chemical and physical modification of AG provides new functionality for the desired application such as drug delivery devices and mimicking tissues for engineering. AG consists of molecules including arabinogalactan, amino acids and short chain arabinose side chains.<sup>9</sup> It has been used as emulsifier and for encapsulating flavours, especially unstable compounds,<sup>10,11</sup> binding agent in tablets processing<sup>12</sup> and also as a release modifier.<sup>13</sup>

AG microgels have been studied by many researchers for the development of delivery devices. Sarika and James synthesized nanogels using AG, gelatin, and aldehyde *via* the inverse-miniemulsion technique. The gelatin serves as a cross linking agent,<sup>14</sup> while Ganie *et al.* formulated nanogels of AG that were non-toxic using acetyl groups and iodine monochloride with the polysaccharide.<sup>15</sup> Farooq *et al.* prepared and modified AG microgels using diethylenetriamine and taurine that were found to be compatible and non-toxic.<sup>6</sup> Researchers have reported that microgels made from AG are degradable, non-toxic and compatible for drug delivery, but AG has poor mechanical strength, is highly soluble in water, and has low viscosity at high concentrations. It is possible to overcome these drawbacks through the modification of AG using a monomer with good mechanical strength, such as methacrylic acid (MAA).<sup>16</sup> Microgels formulated by combination of AG and MAA are hypothesized to improve their mechanical properties, swelling property and controllable viscosity. The present research was targeted on synthesizing MAA modified AG (AGMAA) microgels *via* water in oil emulsion system by cross linking and polymerization reactions. The emulsion technique was applied to promote the formation of spherical shaped particles that are useful for many applications due to their large surface area. The capability of the AGMAA microgels as potential candidate as drug carriers was also evaluated through encapsulation of doxorubicin in the microgels.

## EXPERIMENTAL

Arabic gum (AG) branched polysaccharide ( $M_w$ : 250,000 g mol<sup>-1</sup>, Sigma–Aldrich), methacrylic acid (MAA) ( $M_w$ : 86.06 g mol<sup>-1</sup>, 99 %, Merck), *N,N'*-methylenebisacrylamide (MBA,  $M_w$ : 154.17 g mol<sup>-1</sup>, 99 %, Sigma–Aldrich), poly(ethylene glycol) sorbitan monolaurate (Tween 20), Sigma–Aldrich), ammonium persulfate (APS,  $M_w$ : 228.20 g mol<sup>-1</sup>, Sigma–Aldrich), doxorubicin (Sigma–Aldrich), acetone ( $M_w$ : 58.08 g mol<sup>-1</sup>, 99 %, Merck), hexane ( $M_w$ : 86.18 g mol<sup>-1</sup>, 99 %, Sigma–Aldrich), ethanol (99 %, Sigma–Aldrich), and sodium hydroxide pellets ( $M_w$ : 40.0 g mol<sup>-1</sup>, Schmidt) were used as received without modification.

### *Synthesis of Arabic gum microgel via emulsion polymerization*

Microgels were synthesized according to a previously reported method using the inverse suspension method whereby oil in water emulsion systems was prepared.<sup>8,17,18</sup> A novel oil in water emulsion system consisting of surfactant Tween 20 (10 %) in hexane for the synthesis of AG microgels was applied in this study. A solution of 10 % AG in 0.5 M NaOH solution was prepared and stirred for one hour to form a homogenous solution. Thereafter, 10 ml of the prepared solution was transferred into 100 ml reaction bottle containing 50 ml of the emulsion system of Tween 20 in hexane. The mixture was mixed for 30 min at 1000 rpm using magnetic stirrer, 2 ml of 2.5 % ammonium persulphate solution was added, and stirred for 30 min at 60 °C, followed by the addition of 100 mg *N,N'*-methylene bisacrylamide (MBA) as the crosslinking agent of the polymerization reaction. The colour change of the mixture to whitish indicated the formation of particles through crosslinking. The stirring was continued for additional 30 min to ensure completeness of the reaction. The product was precipitated using excess acetone, the emulsion phase was decanted, and the solid residue of the microgel particles were washed twice with acetone and twice with ethanol:water solution in the ratio of (1:1) by volume. The AG microgels were incubated in an oven at 45 °C before analysis.

### *Synthesis of arabic gum cross-linked methacrylic acid microgel*

Methacrylic acid modified Arabic gum microgels (AGMAA) were synthesized using a similar procedure to that given above with the addition of 2 ml solution of methacrylic acid and left stirring for 30 min before the final addition of 100 mg *N,N'*-methylene bisacrylamide (MBA) to crosslink AG and MAA in the emulsion reaction system. The colour of the mixture changed from colourless to whitish upon formation of the particles. The stirring was continued for an additional 30 min to allow complete crosslinking of the particles.

### *Physicochemical characterization*

*Fourier transform infrared spectroscopy (FTIR).* AG, AGMAA microgels, AGMAA microgel entrapped doxorubicin, physical mixture of AGMAA microgels and doxorubicin, and all the starting materials were analysed using a Perkin Elmer Spectrum 400 at 25 °C. The wavenumber range of 4000–500 cm<sup>-1</sup> at a resolution of 2 cm<sup>-1</sup> was used for the analysis. The background was analysed to serve as a control. The microgels were dried in an oven before the analysis.

*X-Ray diffraction analysis (XRD).* The crystallinity and diffraction pattern of the microgels were analysed using an Empyrean X-ray diffractometer. The samples were exposed to CuK $\alpha$  radiation at an accelerating voltage of 40 kV and a current of 40 mA. The scan rate was set at 1°/min. The diffraction angle was varied within the range of 5 to 50° at 2 $\theta$ . The analysis was performed at 25 °C.

*Differential scanning calorimetry (DSC).* The thermal properties of the microgels were analysed using differential scanning calorimeter (Perkin Elmer). About 7–10 mg of dried mic-

rogel samples was weighed in an aluminium pan while an empty pan was the reference pan. The sample was heated under an nitrogen atmosphere at a scanning rate of 10 °C/min. The measurements were performed within the temperature range of 20–350 °C.

*Field emission scanning electron microscope (FESEM).* The surface morphology of microgels was observed using a field emission scanning electron microscope. The microgels were initially swollen in water for 24 h, followed by freeze drying in liquid nitrogen for 48 h. The dried microgels samples were then coated with gold to prevent charging effect. The morphology was studied with a Quant FEG 450 instrument at a beam voltage of 5 kV. Surface images were captured at different magnifications and focus.

#### *Hydrodynamic particle size and zeta potential measurement*

The analysis of the mean particle size and zeta potential of AG and AGMAA microgels were measured using a Malvern Nano ZS Zetasizer Zen 3600 (Malvern Instruments Ltd., UK).<sup>19</sup> The samples were investigated at a backscattered angle of 173° using a scattering laser light 633 nm at 25 °C. The mean particle size and zeta potential were obtained from three replicates.

#### *Degradation study of microgels*

The microgels were swollen in phosphate buffer solution (PBS) of pH 7.4 for the degradation study at temperature 37 °C. The degradability of AG and AGMAA microgels were analysed. This enable assessing the effect of the cross-linked monomers on the rate of degradation of the microgels at pH 7. The microgels particles were first dried in oven to constant weight followed by immersion into 20 ml of aqueous buffer solutions at 37 °C for six weeks.<sup>20</sup> The weight of AG and AGMAA microgels particles were recorded every 24 h and the aqueous medium was replaced by fresh buffer solutions pre-equilibrated at 37 °C every 24 h throughout a period of six weeks.

The weight loss percentage or decrease in mass percentage was recorded as percentage degradation of the microgel materials as a function of time, as shown in Eq. (1):

$$\text{Degradation} = 100 \frac{M_t}{M_{\max}} \quad (1)$$

where  $M_t$  is the weight at time  $t$  and  $M_{\max}$  is the maximum swollen weight of the microgel.

#### *Doxorubicin encapsulations and in vitro drug release study*

The post-formation loading method was applied to entrap 3 mg doxorubicin in the formulated microgel. The encapsulation efficiency of the microgel was studied by measuring 300 mg of the dried microgel and added it into 30 ml doxorubicin solution of concentration 0.1 mg ml<sup>-1</sup>. The mixture solution was placed on an orbital shaker at 25 °C under a constant shaking of 10 rpm for 24 h to ensure efficient encapsulation of the doxorubicin into the microgels. The entrapped doxorubicin in microgel was separated from the un-entrapped doxorubicin by centrifugation at 10,000 rpm for 10 min. The supernatant was collected for determination of the concentration of un-entrapped doxorubicin. The microgel samples were dried in an oven at 45 °C. The encapsulation efficiency of the doxorubicin was determined according to Eq. (2), where  $c_{\text{TDS}}$  represented the concentration of doxorubicin that was initially introduced into the preparation,  $c_{\text{DS}}$  is the concentration of drugs left in the supernatant after the centrifugation. A series of doxorubicin in deionized water varying in concentration were prepared as standards for the calibration curve and measured at 485 nm using a UV–Vis spectrophotometer:

$$EE = 100 \frac{c_{\text{TDS}} - c_{\text{DS}}}{c_{\text{TDS}}} \quad (2)$$

The *in vitro* drugs release from the microgels with different loading capacity was investigated in mediums of pH 4.2 and pH 7.4. The study of drug release at pH 4.2 was performed to assess the drug release and kinetics in acidic medium while pH 7.4 represent a neutral pH. All the studies were performed at a temperature of 37 °C.

The kinetic of drug released was studied using the Ritger–Peppas model<sup>21</sup> as one of the most appropriate models used for hydrogels and microgel drug release study, where the ratio of drug release is directly proportional to time as shown in Eq. (3):

$$F_D = \frac{m_t}{m_\infty} = kt^n \quad (3)$$

where  $F_D$  is the ratio of drug release at time  $t$ , to the equilibrium swollen state.  $m_t$  and  $m_\infty$  are the amount of drugs released at time  $t$  and at equilibrium state, respectively.  $n$  is the diffusion exponent of the release mechanism and  $k$  is the proportionality constant that measures the speed of release and geometrical parameters comparable to the drug-polymer system.

## RESULTS AND DISCUSSION

### *Synthesis of AG microgels via emulsion polymerization*

The emulsion system consisting of 10 % of aqueous Tween 20 in hexane enabled the formation of reversed micelle to accommodate Arabic gum molecules in the core of reversed micelle that are hydrophilic.<sup>8,17</sup> Addition of APS generated free radical during heating at temperature ≈60 °C to create active sites on the Arabic gum molecules. Addition of MBA into the emulsion system under constant stirring allowed the diffusion of the MBA molecules into the core of the reversed micelles. Subsequently, MBA cross-linked with the molecular radical active site of the hydroxyl group in Arabic gum molecules to terminate the reaction. Tween 20 as a surfactant remained in the structure to provide a template for the formation of microgels.<sup>22</sup>

### *Formulation of Arabic gum-grafted-poly(methacrylic acid) microgels*

A similar reaction occurred between AG and MAA as in the formation of AG microgel, except that MAA was introduced into the reaction after the generation of AG radicals. The AG radical abstracted a proton from the ethylene group of methacrylic acid leading to propagation of the polymer chains<sup>23–25</sup> through graft polymerization to form the Arabic gum–grafted-poly(methacrylic acid). Then, the cross-linking agent (MBA) was added into the emulsion system to terminate the chain propagation. In the termination reaction, MBA cross-linked the molecules of AG with radical active hydroxyl group and the radical active ethylene group of poly(methacrylic acid). The proposed scheme is shown in the graphical abstract while the digital images of the products are shown in Fig. 1.

### *FTIR spectroscopy*

The FTIR spectrum of starting materials and the synthesized microgels are shown in Fig. 2. The AG spectrum indicates the presence of peaks at 3279 (OH), 2928 (CH stretch), 1601 (C=O group), 1410 (CH<sub>2</sub> group) and 1026 cm<sup>-1</sup> (CO



Fig. 1. Digital images of :a) AG microgels and b) AGMAA microgels.

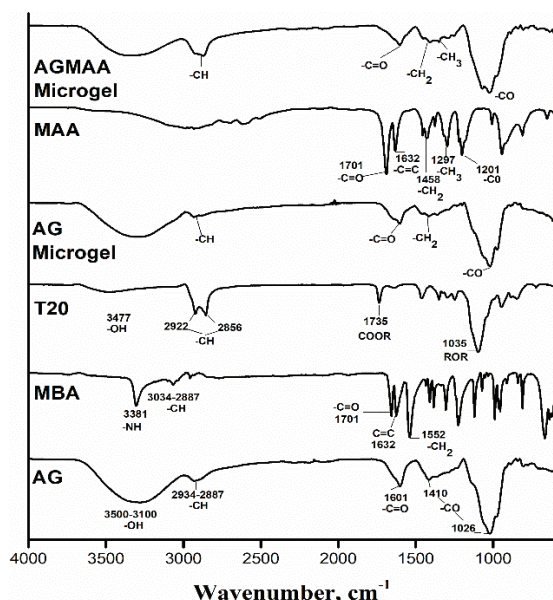


Fig. 2. FTIR Spectra of AG, MBA, T20, AG microgel, MAA and AGMAA microgel.

group). The Tween 20 spectrum shows the presence of hydrogen bonded O–H stretching at 3477 cm<sup>-1</sup>, asymmetric and symmetric methylene stretching vibration at 2922 and 2856 cm<sup>-1</sup>, carbonyl group from R–CO–O–R at 1734 cm<sup>-1</sup> and ether linkages of polyethylene glycol (–CH<sub>2</sub>–O–CH<sub>2</sub>–) as a sharp peak at 1092 cm<sup>-1</sup>. The AG microgel spectrum indicates a broad peak at 3302 cm<sup>-1</sup> of NH and OH stretching due to their overlapping and the peaks at 2928, 1605 and 1026 cm<sup>-1</sup> correspond to C–H stretching, C=O group and CO stretch, respectively. The low intensity but visible peaks in the range of 900–1150 cm<sup>-1</sup> correspond to the ethylene group indicates the presence of Tween 20 in the microgel.

The spectrum of the AGMAA microgels shows peaks at 3302 (OH/NH stretch), 2928 (CH stretch), 1601 (C=O), 1434 (–CH<sub>2</sub> group), 1303 (–CH<sub>3</sub> group) and 1026 cm<sup>-1</sup> (C–O stretch). The disappearance of the peak at 1632 cm<sup>-1</sup> (C=C group) indicated the successful grafting of AG and MAA molecules in the mic-

rogel. The presence of Tween 20 in the microgel was identified by the band at  $1100\text{ cm}^{-1}$ , correspond to  $-\text{CH}_2\text{--O--CH}_2-$  group.

The interaction between doxorubicin and AGMAA microgels at the level of functional groups was evaluated using the FTIR spectrum as shown in Fig. 3. The spectrum of doxorubicin showed characteristic absorption bands at  $3309\text{ (N--H asymmetric stretching)}$ ,  $2920\text{ (C--H stretching)}$ ,  $1731\text{ (C=O symmetric stretching)}$ ,  $1617$  and  $1578\text{ (amide I and amide II, respectively)}$ ,  $1285\text{ (O--H--O)}$ , and  $991\text{ cm}^{-1}$  ( $=\text{C--H bending}$ ).<sup>26,27</sup> AGMAA microgel entrapped doxorubicin showed characteristic bands at  $3280\text{ (OH/NH stretch)}$ ,  $2935\text{ (CH stretch)}$ , broadening band at  $1624\text{ (C=O an--1 (C--O stretch) that can be attributed to AGMAA microgel. On the other hand, the presence of bands at }1539\text{ cm}^{-1}$  (amide II), and the characteristic band for doxorubicin at  $1286\text{ cm}^{-1}$  also noticed, this indicated the presence of doxorubicin molecules in the AGMAA microgels. The spectra of AGMAA microgel entrapped doxorubicin was found approximately similar to that of the physical mixture. The absence of a new peak in the physical mixture suggested that there was no chemical interaction between doxorubicin and the AGMAA microgel. This demonstrated the integrity and stability of DOX within the AGMAA microgel.

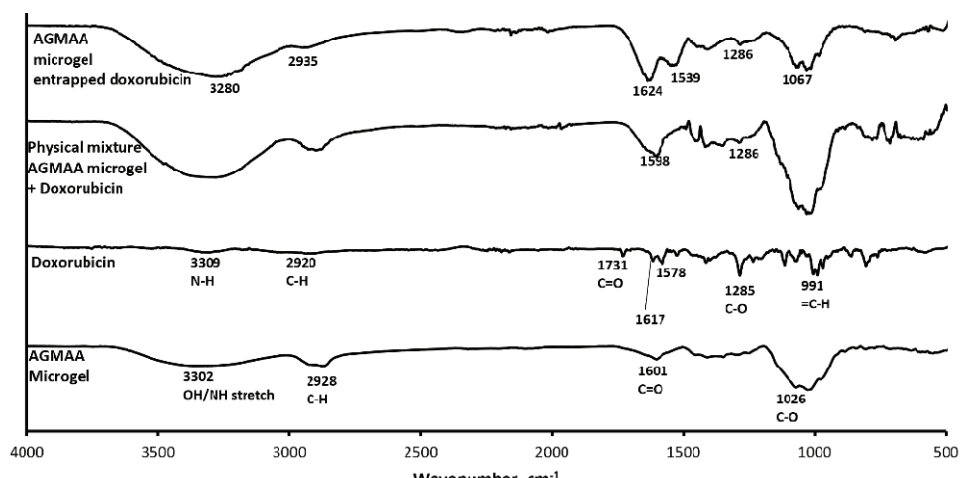


Fig. 3. FTIR Spectra of AGMAA microgel, Doxorubicin, physical mixture of AGMAA microgel + doxorubicin, and AGMAA microgel entrapped doxorubicin.

#### Differential scanning calorimetry (DSC)

The thermograms of AG and AGMAA microgels are shown in Fig. 4. Two major curves were observed in the thermogram, one endothermic and one exothermic. The endothermic curves correspond to the melting temperature of microgels that appeared at  $183$  and  $171\text{ }^{\circ}\text{C}$  for AG and AGMAA, respectively. The

microgels changed phase from solid to liquid state. These data were found similar to AG microgels by Farooq *et al.* and AGMAA hydrogels by Mamman *et al.*<sup>6,16</sup> The melting enthalpy of the Arabic gum microgel was higher ( $152 \text{ J g}^{-1}$ ) than that of the AGMAA microgel ( $139 \text{ J g}^{-1}$ ). The lower melting peak and melting enthalpy for AGMAA microgels could be attributed to the formation of branches by MAA in the AG molecules. The ordered arrangement of the AG was disrupted by grafting with MAA molecules, this relaxed the stiffness of the molecular arrangements in the AG molecules. The exothermic curves at 277 and 290 °C for AG and AGMAA microgels, respectively, indicate decomposition of the microgels. The decomposition enthalpy for AG and AGMAA microgels were  $-25.4$  and  $-149 \text{ J g}^{-1}$ , respectively. The difference in temperature and enthalpies of decomposition suggests the grafting of MAA on AG stabilized the formulated microgels.

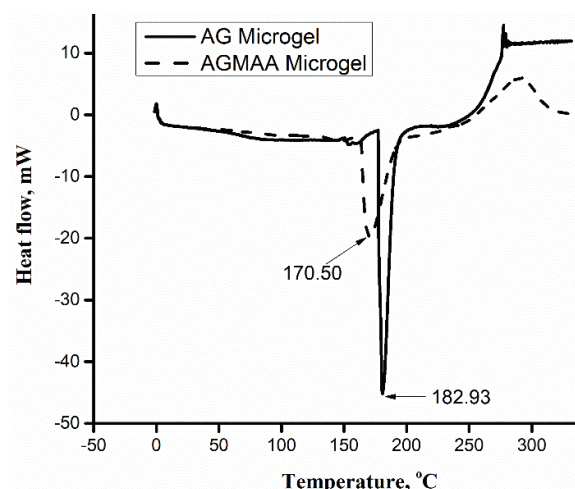


Fig. 4. DSC thermograms of AG and AGMAA microgels.

#### X-Ray diffraction

The XRD plots of the AG and AGMAA microgels are presented in Fig. 5. The XRD of the AG microgel showed the presence of two characteristics peaks at  $2\theta = 14$  and  $20^\circ$ . The first peak was sharp with a low peak area confirming the unique structural reformation due to cross-linking of the AG particles while the latter peak was broad with a low intensity is usually found as a characteristic peak of Arabic gum but with high intensity as amorphous polymer.<sup>16</sup> The distinctive sharp peak of the AG microgel indicates the absence of modifying agents and regularity in the newly formed semi-crystalline structure with a characteristic sharp peak at  $2\theta = 14^\circ$ . The AGMAA microgels showed a reflection peak at  $2\theta = 20^\circ$ . The semi-crystal nature of the gum was reduced due to the introduction of MAA monomers into the main structure.

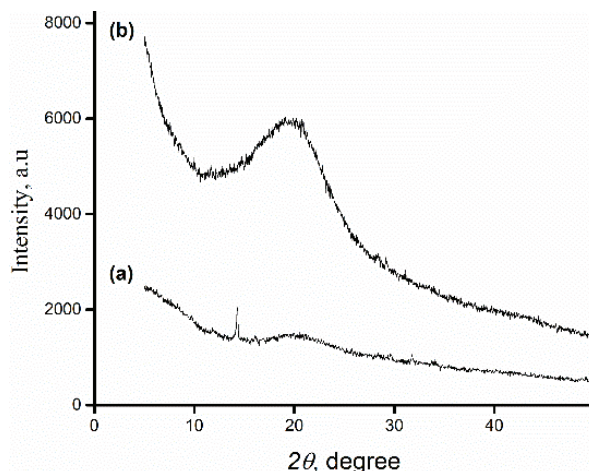


Fig. 5. XRD Spectrum of the microgels: a) Arabic gum microgel and b) AGMAA microgel.

#### *Field emission scanning electron microscopy (FESEM)*

The micrographs of the AG microgel and AGMAA microgel are shown in Fig. 6. The particles are spherical because the microgels were formed within the spherical shape micelles during polymerization, the system where the processes of grafting and cross-linking occurred.<sup>6,26</sup> The micrograph of AG microgels is shown in Fig. 6a. It shows the presence of uniform and closely packed spherical microgels from the inner point of view. While Fig. 6b shows the micrograph of AGMAA microgel, the morphology shows the presence of many spherical structures that are not as closely packed as the AG microgels.

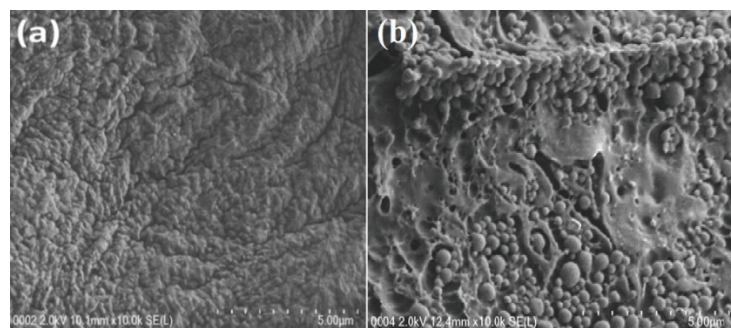


Fig. 6. FESEM micrographs of: a) AG microgel and b) AGMAA microgel.

#### *Particle size and potential analysis*

The average range of the particle size distribution by number of the AG microgel was smaller than the size of the methacrylic acid modified AGMAA microgels. The AG and AGMAA microgels have particle size ranges of 1.0–7.0

and 0.7–7.5  $\mu\text{m}$ , respectively. The particles size depends on the amount of surfactant introduced in the emulsion system and agrees with AG microgels synthesized by other researchers.<sup>6,18</sup> A subsequent study was conducted by reducing the amount of surfactant from 10 % as stated in the synthesis procedure to 5 % in order to determine the effect of the surfactant on the size of the microgel particles and it was found that the size of the microgels has a direct relation with the emulsion system. This is shown in Fig. 7a and b where the size is shown to increase as the surfactant concentration is increased.

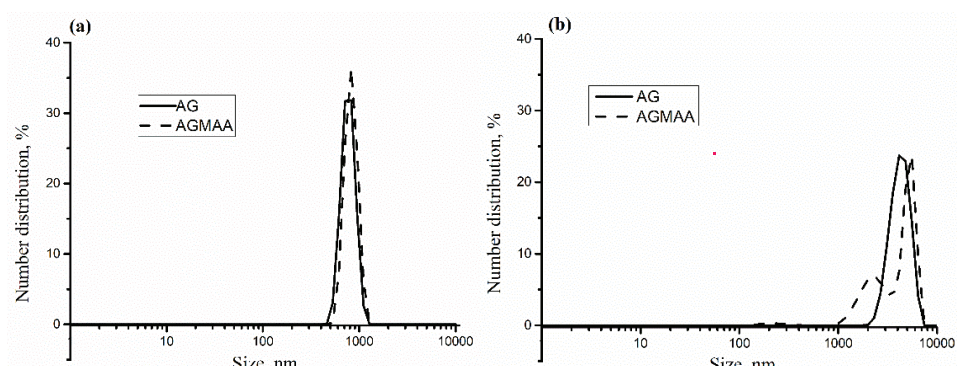


Fig. 7. Microgel particles sizes of AG and AGMAA microgels at: a) 5 and b) 10 % surfactant.

The zeta potential, conductivity, and electrophoretic mobility (velocity per field strength) of the microgels are given in Table I. The magnitude of zeta potential for AGMAA microgels are significantly more negative as compared to the AG microgels. AG microgels displayed a lower magnitude of the zeta potential ( $-21.5 \text{ mV}$ ) compared to AGMAA microgels ( $-48.5 \text{ mV}$ ). AGMAA microgels showed the highest magnitude of the zeta potential, possibly attributed to ionization<sup>28</sup> of the methacrylic acid monomers in the polymer chain resulting in the presence of anions surrounding the surface.<sup>28</sup>

TABLE I. Zeta potential, conductivity and electrophoretic mobility of the microgels

Microgel	Zeta potential, mV	Conductivity, $\text{mS cm}^{-1}$	Electrophoretic mobility, $\mu\text{m cm V s}^{-1}$
AG	-21.5	3.9	-1.7
AGMAA	-48.5	1.9	-3.8

#### *Degradation study of the microgels*

The degradation study of the microgels was only performed in phosphate buffer solution pH 7.4, the microgel samples were immersed in the medium and the AG microgel swelled to maximum size in three days. There was a significant loss of weight/degradation of the AG microgel to 88 % after four days immersion in the medium. It continued to degrade until only 36 % of its weight remained

after thirteen days. On the following day, there was a drastic decrease of weight from 36 to 18 % and subsequently to 4 % after fifteen days and further reduced to 0.01 % on the subsequent day. Complete 100 % degradation of the Arabic gum crosslinked microgel had occurred after the seventeenth days. On the contrary, for the AGMAA microgels, the maximum swelling in the phosphate buffer solution pH 7.4 was achieved in two days. The microgels started to degrade after three days and down to 51 % in twenty-eight days. The modified microgel particles continued to degrade and only 2 % of the initial microgel weight was left after 36 days immersed in the medium. In conclusion, about 98 % of the AGMAA microgel was degraded in 36 days. Degradation depended solely on the structural composition of each microgel sample, AG microgel which degrade faster and has highest percentage degradation is as the result of the availability of carboxylic group and lack of synthetic materials such as the monomers and cross-linking agents while the slow degradation rate observed in AGMAA microgels could be attributed to the presence of synthetic monomers of methacrylic acid and high cross-linking between the carboxylic group of AG molecules and ethylene group of the methacrylic acid.<sup>16</sup> The degradation is shown graphically in Fig. 8.

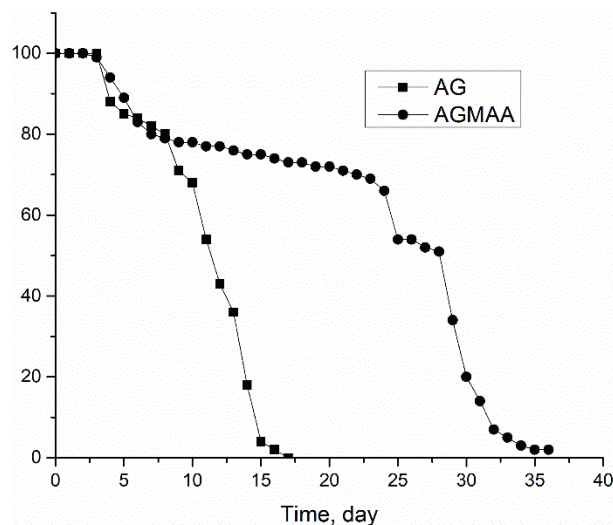


Fig. 8. Degradation of AG microgels and AGMAA microgels in phosphate buffer pH 7.4; the values at y-axis relate to content of residuals in %.

#### Drug encapsulation

The post-formation loading method was used to entrap doxorubicin in microgels to study the potential of formulated microgels as drug carrier. The concentration of doxorubicin entrapped in the microgels were determined from the calibration curve. The encapsulation efficiency of the AG microgel was  $61.3 \pm 0.3$  %

that was lower than AGMAA microgel  $73.4 \pm 0.3\%$ . Drug encapsulation on microgels depends on the swelling capacity on absorption. The high percentage encapsulation by AGMAA microgel is ascribed to the high swelling rate of the microgels compare the AG microgels.

#### In vitro drug release study

The *in vitro* release profile of doxorubicin drug from the AG microgels and AGMAA microgels in buffer solutions of pH 4.2 and pH 7.4 at 37 °C are shown in Fig. 9. The *in vitro* drug release from the microgel formulations is dependent on the medium of release and the microgel formulation. The percentage release in acidic medium (pH 4.2) for all the formulations was higher as compared to the release in pH 7.4.

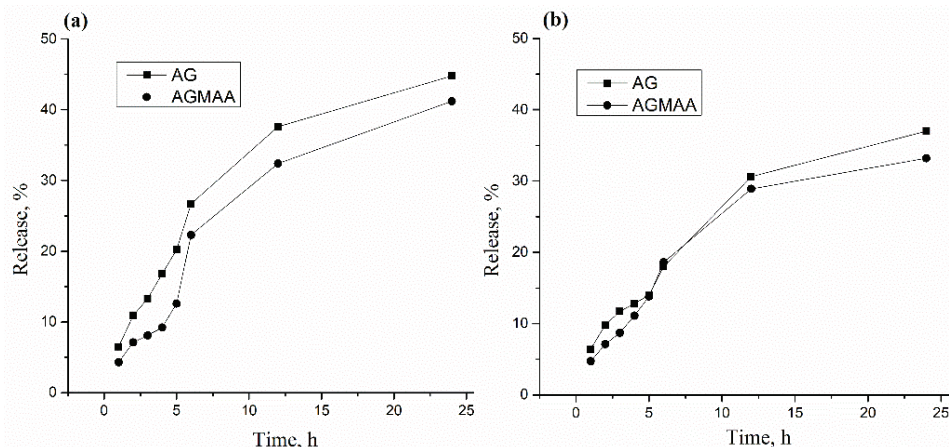


Fig. 9. Release of doxocubicin from microgels at pH: 4.2 (a) and 7.4 (b).

A high rate of release was recorded in all the media within the first 5 h, and this could be credited to the presence of doxorubicin drugs that are loosely attached to the microgel particles after the centrifugation process. AG and AGMAA have a percentage release of 44.8 and 41.3 % in pH 4.2 and 37.0 and 33.2 % in pH 7.4, respectively. The lower release at high pH is attributable to the restriction of protonation of the carboxylic group at higher pH by the presence of the surfactant molecules on the microgels surfaces leading to a low rate of network expansion.

The *in vitro* release kinetics of the microgels were investigated using the Ritger-Peppas model and the data generated for the kinetics were fitted and the kinetics data such as diffusion exponent ( $n$ ) for the mechanism of drug release and the geometry parameter constant ( $k$ ) for the velocity of drug release that is analogous to a polymer-drug system were calculated and the results are given in Table II. The kinetics data at pH 4.2 and pH 7.4 were different that is due to the

swelling and interaction of the microgels molecules at the different pH values. The value of  $n$  for AG and AGMAA microgels were 0.58 and 0.71 at pH 4.2 and 0.53 and 0.60 at pH 7.4, respectively.

TABLE II. Release kinetics of doxorubicin from microgels at pH 4.2 and 7.4 (values separated by /)

Microgel	$n$	$k \times 10^{-4}$ , h <sup>-n</sup>	$R^2$	$r$
AG	0.58/0.53	6.1/6.0	0.87/0.85	0.93/0.92
AGMAA	0.71/0.60	6.8/6.4	0.89/0.87	0.94/0.93

The observed  $n$  values that are greater than 0.43 but less than 0.85 indicate non-Fickian diffusion mechanism controlled by swelling and diffusion drug release mechanism. The value of the geometry parameter  $k$  for the release velocity was lowered at the high pH indicating a slower rate of drug release at pH 7.4 for the microgel formulations. The values of the statistical parameters such as  $R^2$  and Pearson ( $r$ ) indicate good fitting of the generated data to the Ritger-Peppas model.

#### CONCLUSIONS

The concentration of the surfactant plays an important role on the microgel formation process and affects the size (hydrodynamic diameter) distribution by number of the synthesized microgels. The synthesis of Arabic gum methacrylic acid modified microgel showed a significant improvement in terms of the size, zeta potential and the mechanical strength. Swelling and degradation study indicate a higher rate of degradation for the AG microgels as compared to the AGMAA microgels. These results demonstrated the possibility of microgel formation with improved strength and functionality using microemulsion polymerization method, and the microgel could be used for biomedical and pharmaceutical applications, especially in drug delivery, due to their tunable properties with the required size and surface area for catalytic reactions.

*Acknowledgement.* The research work was supported by University of Malaya, Malaysia. It was financially supported by RU Grant (ST042-2020).

#### ИЗВОД

СИНТЕЗА И ФИЗИЧКО-ХЕМИЈСКА КАРАКТЕРИЗАЦИЈА МИКРОГЕЛА ГУМАРАБИКЕ  
МОДИФИКОВАНЕ МЕТАКРИЛНОМ КИСЕЛИНОМ КАО ПОТЕНЦИЈАЛНОГ  
НОСАЧА ЛЕКОВА

SANI M. IBRAHIM<sup>1,2</sup>, MISNI MISRAN<sup>1</sup> и YIN YIN TEO<sup>1</sup>

<sup>1</sup>Department of Chemistry, Faculty of Sciences, University of Malaya, Kuala Lumpur, Malaysia and

<sup>2</sup>Department of Chemistry, Faculty of Sciences, Federal College of Education, Zaria, Nigeria

Микрогелови полимера угљених хидрата су нетоксични и биокомпатибилни и могу се лако користити у примени за испоруку лекова, медицини и фармацији. Овај рад је показао синтезу микрогела гумарабике (AG) и микрогел гумарабике модификоване метакрилном киселином (AGMAA) користећи технику емулзионе полимеризације вода

у уљу са Tween 20 као површински активним средством и хексаном као растворачем. Микрогелови су окарактерисани коришћењем различитих физичко-хемијских анализа, као што је инфрацрвена спектроскопија са Фуријеовом трансформацијом, термичка стабилност диференцијалном скенирајућом калориметријом, дифракцијом рендгенских зрака, морфологија помоћу скенирајућег електронског микроскопа, док је динамично расипање светlostи коришћено за анализу величине и зета потенцијала. Степен деформације је био већи у микрогелу гумарабику у поређењу са микрогелом гумарабику модификованим метакрилном киселином. Утврђено је да су величина честица и зета потенцијал микрогела гумарабике модификована метакрилном киселином већи и негативнији од микрогела гумарабике. Утврђено је да величина честица микрогела и зета потенцијали зависе од количине метакрилне киселине као агенса за модификацију. Микрогелови су инкапсулирани са доксорубицином методом бubreња и *in vitro* ослобађање је проучавано у медијуму са pH 4,2 и 7,4. Резултати указују на могућност примене ових микрогелова за испоруку лекова.

(Примљено 9. септембра 2021, ревидирано 18. фебруара, прихваћено 21. фебруара 2022)

#### REFERENCES

1. G. Ciofani, S. Del Turco, A. Rocca, G. De Vito, V. Cappello, M. Yamaguchi, X. Li, B. Mazzolai, G. Basta, M. Gemmi, *Nanomedicine* **9** (2014) 773 (<https://www.futuremedicine.com/doi/pdfplus/10.2217/nnm.14.25>)
2. J. K. Oh, D. I. Lee, J. M. Park, *Prog. Polymer Sci.* **34** (2009) 1261 (<https://doi.org/10.1016/j.progpolymsci.2009.08.001>)
3. H. Jing, J. Shi, P. Guoab, S. Guan, H. Fu, W. Cui, *Colloids Surfaces, A* **611** (2021) 125805 (<https://doi.org/10.1016/j.colsurfa.2020.125805>)
4. P. M. Outuki, L. M. B. de Francisco, J. Hoscheid, K. L. Bonifácio, D. S. Barbosa, M. L. C. Cardoso, *Colloids Surfaces, A* **499** (2016) 103 (<https://doi.org/10.1016/j.colsurfa.2016.04.006>)
5. T. S. Anirudhan, J. Parvathy, A. S . Nair, *Carbohyd. Polym.* **136** (2016) 1118 (<https://doi.org/10.1016/j.carbpol.2015.10.019>)
6. M. Farooq, S. Sagbas, M. Sahiner, M. Siddiq, M. Turk, N. Aktas, N. Sahiner, *Carbohyd. Polym.* **156** (2017) 380 (<https://doi.org/10.1016/j.carbpol.2016.09.052>)
7. J. Jacob, J.T. Haponiuk, S. Thomas, S. Gopi, *Mat. Today Chem.* **9** (2018) 43 (<https://doi.org/10.1016/j.mtchem.2018.05.002>)
8. S. Sagbas, N. Sahiner, *Carbohyd. Polym.* **200** (2018) 128 (<https://doi.org/10.1016/j.carbpol.2018.07.085>)
9. A. S. Hoffman, *Adv. Drug Deliv. Rev.* **64** (2012) 18 (<https://doi.org/10.1016/j.addr.2012.09.010>)
10. A. Romo-Hualde, A. I. Yetano-Cunchillos, C. González-Ferrero, M. J. Sáiz-Abajo, C. J. González-Navarro, *Food Chem.* **133** (2012) 1045 (<https://doi.org/10.1016/j.foodchem.2012.01.062>)
11. D. Verbeken, S. Dierckx, K. Dewettinck, *App. Microbiol. Biotech.* **63** (2003) 10 (<https://doi.org/10.1007/s00253-003-1354-z>)
12. T. R. Bhardwaj, M. Kanwar, R. Lal, A. Gupta, *Drug Dev. Ind. Pharm.* **26** (2000) 1025 (<https://doi.org/10.1081/DDC-100100266>)
13. N. Malviya, S. Jain, S. Malviya, *Acta Pol. Pharm.* **67** (2010) 113 ([https://ptfarm.pl/pub/File/acta\\_pol\\_2010/2\\_2010/113-118.pdf](https://ptfarm.pl/pub/File/acta_pol_2010/2_2010/113-118.pdf))

14. P. R. Sarika, N.R. James, *Int. J. Biol. Macromol.* **76** (2015) 181 (<https://doi.org/10.1016/j.ijbiomac.2015.02.038>)
15. S. A. Ganie, A. Ali, N. Mazumdar, *Carbohyd. Polym.* **129** (2015) 224 (<https://doi.org/10.1016/j.carbpol.2015.04.044>)
16. I. S. Mamman, Y. Y. Teo, M. Misran, *Polym. Bull.* **78** (2021) 3399 (<https://doi.org/10.1007/s00289-020-03267-4>)
17. S. Sagbas, S. Butun, N. Sahiner, *Carbohyd. Polym.* **87** (2012) 2718 (<https://doi.org/10.1016/j.carbpol.2011.11.064>)
18. P. Ilgin, G. Avci, C. Silan, S. Ekici, N. Aktas, R. S. Ayyala, V. T. John, N. Sahiner, *Carbohyd. Polym.* **82** (2010) 997 (<https://doi.org/10.1016/j.carbpol.2010.06.033>)
19. Y. Y. Teo, M. Misran, K. H. Low, *J. Chem.* **9** (2012) 421286 (<https://doi.org/10.1155/2012/421286>)
20. R. A. McBath, D. A. Shipp, *Polym. Chem.* **1** (2010) 860 (<https://doi.org/10.1039/C0PY00074D>)
21. P. L. Ritger, N.A. Peppas, *J. Control. Rel.* **5** (1987) 23 ([https://doi.org/10.1016/0168-3659\(87\)90034-4](https://doi.org/10.1016/0168-3659(87)90034-4))
22. B. Wedel, T. Brändel, J. Bookhold, T. Hellweg, *ACS Omega* **2** (2017) 84 (<https://doi.org/10.1021/acsomega.6b00424>)
23. W. Gao, C. Li, J. Li, Q. Zhang, N. Wang, B. Abdel-Magid, X. Qu, *J. Adh. Sci. Tech.* **33** (2019) 2031 (<https://doi.org/10.1080/01694243.2019.1625852>)
24. N. A. Harun, S. Kassim, S. T. Muhammad, F. E. Rohi, N. N. Norzam, N. S. M. Tahier, *AIP Conf. Proc.* **1885** (2017) 020032 (<https://doi.org/10.1063/1.5002226>)
25. J. X. Zhong, J. R. Clegg, E. W. Ander, N. A. Peppas, *J. Biomed. Mat. Res., A* **106** (2018) 1677 (<https://doi.org/10.1002/jbm.a.36371>)
26. S. Kayal, R. V. Ramanujan, *Mater. Sci. Eng.* **30** (2010) 484 (<https://doi.org/10.1016/j.msec.2010.01.006>)
27. D. Matyszewska, E. Napora, K. Źelechowska, J. F. Biernat, R. Bilewicz, *J. Nanopart. Res.* **20** (2018) 143 (<https://doi.org/10.1007/s11051-018-4239-x>)
28. L. Chang, J. Liu, J. Zhang, L. Deng, A. Dong, *Polym. Chem.* **4** (2013) 1430 (<https://doi.org/10.1039/C2PY20686B>)
29. S. M. North, S. P. Armes, *Polym. Chem.* **11** (2020) 2147 (<https://doi.org/10.1039/D0PY00061B>).